DOI: 10.1002/ejic.201000585

Synthesis, Characterization and Luminescence Properties of Dipyridin-2-ylamine Ligands and Their Bis(2,2′-bipyridyl)ruthenium(II) Complexes and Labelling Studies of Papain from *Carica papaya*

Pierre Haquette,[a] Julien Jacques,[a] Samuel Dagorne,[b] Céline Fosse,[c] and Michèle Salmain*[a]

Keywords: Luminescence / Ruthenium / Protein modifications / Circular dichroism / Thiol labels

Two luminescent polypyridyl Ru^{II} complexes including dipyridin-2-ylamine (dpa) ligands functionalized by a maleimide group, namely $[Ru(bpy)_2(\mathbf{1a–b})](PF_6)_2$ (bpy = 2,2′-bipyridyl; **1a** = 1-[4-(dipyridin-2-ylamino)butyl]-1*H*-pyrrole-2,5-dione; **1b** = 1-[5-(dipyridin-2-ylamino)pentyl]-1*H*-pyrrole-2,5-dione), were synthesized, and the X-ray structure of $[Ru(bpy)_2(\mathbf{1b})](PF_6)_2$ was solved. The photophysical properties of these complexes and the starting dipyridin-2-ylamine ligands were studied. Upon excitation at their maximum of absorption, the dpa ligands exhibited weak luminescence because of quenching by the maleimide group. Conversely, the complexes displayed noticeable luminescence, with an emission wavelength at 600 nm that originated from a metal-to-ligand charge-transfer (MLCT) triplet state. Reaction of the ligands and the complexes with the cysteine endoproteinase papain was shown to occur at the single free cysteine (Cys25) as expected by the usual reactivity of maleimides. The resulting bioconjugates displayed luminescence assigned to the attached fluorophore, and luminescence enhancement was observed with respect to the starting reagents. The circular dichroism spectrum of one of the papain–Ru^{II} bioconjugates displayed a typical bisignate band in the near-UV range, indicating that the reaction of papain with the *rac* complex appeared to be stereoselective in favour of the Δ enantiomer.

Introduction

Polypyridyl complexes of ruthenium(II) and other transition metals like rhenium(I), iridium(III) and osmium(II) are known to display quite unique luminescence properties.[1] Excitation at the metal-to-ligand charge-transfer (MLCT) transition induces light emission characterized by large Stokes' shifts and long decay times.[2] Combined with their ability to bind to DNA, some polypyridyl Ru^{II} complexes have also been shown to induce DNA photocleavage.[3] In order to be analytically or chemically useful, these probes must be derivatized to enable their attachment to biomolecules such as proteins. Thiols are particularly useful targets as there are generally only a few free sulfhydryl groups in proteins. Alternatively, cysteine residues can be genetically engineered at defined locations to fit the purpose. Maleimide derivatives are well suited to introduce reporter groups into proteins as they are known to react quite selectively with thiols at neutral pH to yield stable thioethers by Michael addition to the double bond of the maleimide ring.[4] A few polypyridyl complexes of Ru^{II} targeting thiols have previously been reported in the literature[5–7] as well as several Re^{I} complexes,[8] but none of them contain the dipyridin-2-ylamine (dpa) motif.

We recently reported the synthesis of the dipyridin-2-ylamine ligands **1a** and **1b** (Scheme 1) in which the amine nitrogen atom carries a 4- or 5-carbon aliphatic chain terminated by a maleimide moiety. Reaction with the dimeric complexes $[(\eta^6\text{-arene})RuCl_2]_2$ (arene = benzene or *p*-cymene) yielded the monomeric cationic complexes $[(\eta^6\text{-arene})Ru(\mathbf{1a–b})Cl]Cl$. These complexes have been used to introduce $(\eta^6\text{-arene})Ru^{II}$ species into the cysteine endoproteinase papain by reaction with the single free cysteine residue (Cys25) located in the enzyme's active site.[9] Subsequently, one of the resulting metallopapain derivatives was shown to catalyse a Diels–Alder reaction in aqueous medium at low catalyst loading.[10] In order to gain further insight into the interaction between papain and these complexes once they are bound to the active site, we synthesized other dpa complexes of Ru^{II}, namely $[Ru(bpy)_2(\mathbf{1a–b})](PF_6)_2$ (**3a–b**), with potentially useful photophysical properties {the $[(\eta^6\text{-arene})Ru(\mathbf{1a–b})Cl]Cl$ complexes have no particular physicochemical properties that could be exploited for this purpose}. The molecular structures of three complexes were solved by X-ray crystallography. Their reactivity with pa-

[a] Chimie ParisTech (Ecole Nationale Supérieure de Chimie de Paris), Laboratoire Charles Friedel, CNRS UMR 7223,
11 rue Pierre et Marie Curie, 75231 Paris, France
Fax: +33-1-44276732
E-mail: michele-salmain@chimie-paristech.fr
[b] Laboratoire DECOMET, Institut de Chimie, UMR CNRS 7177, Institut Le Bel,
4 rue Blaise Pascal, 67000 Strasbourg, France
[c] Chimie ParisTech (Ecole Nationale Supérieure de Chimie de Paris), Laboratoire de Spectrométrie de Masse,
11 rue Pierre et Marie Curie, 75231 Paris, France

Supporting information for this article is available on the WWW under http://dx.doi.org/10.1002/ejic.201000585.

pain was studied, and the photophysical properties of the ligands and complexes alone and once conjugated to the protein were delineated.

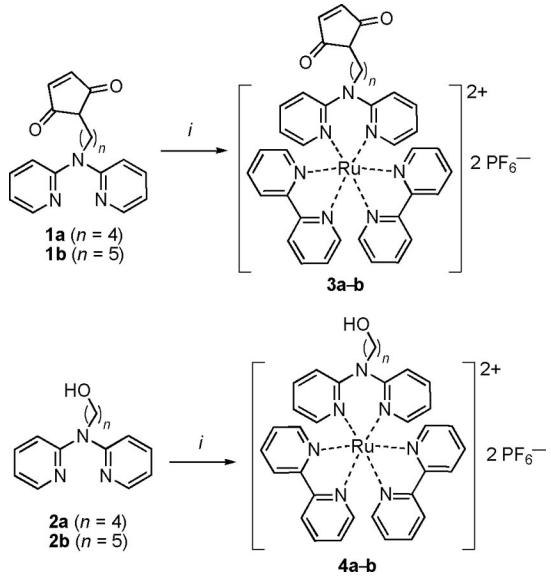

Scheme 1. (i) $[Ru(bpy)_2Cl_2]$ in EtOH, Δ, 16 h, then $NaPF_6$.

Results and Discussion

Synthesis

Ligands **1a**–**b** and **2a**–**b** were synthesized according to our previously described procedure.[9] Complexes **3a**–**b** and **4a**–**b** were obtained in high yield by reaction of ligands **1a**–**b** or **2a**–**b** with $[Ru(bpy)_2Cl_2]$ in EtOH at reflux (Scheme 1). The four complexes were fully characterized by ^1H and ^{13}C NMR spectroscopy and HR mass spectrometry.

X-ray and NMR Spectroscopic Characterization of Ru^{II} Complexes

The molecular structures of **3a**, **4a** and **4b** were established by single-crystal X-ray analysis. Diffraction-quality crystals were grown by slow diffusion of *n*-hexanes into concentrated CH_2Cl_2 solutions of the complexes. The crystallographic data are given in Table S1, whereas selected bond lengths and angles are given in Table S2. ORTEP drawings with the atomic numbering scheme are shown in Figure 1. Complexes **3a**, **4a** and **4b** crystallized in the $P\bar{1}$ triclinic space group with one molecule of dichloromethane. The three structures are rather similar with the metal atom exhibiting a distorted octahedral N_6 coordination sphere. The dpa ligand is bound to the metal atom through the two pyridyl nitrogen atoms. The metal–nitrogen bond lengths range from 2.048(5) to 2.091(4) Å. The N–Ru–N angles from the bpy ligands ranging from 78.69(11) to 78.81(17)° are close to those of a regular octahedral geometry, whereas the N–Ru–N angles from the dpa ligands are larger, ranging from 85.69(18) to 86.42(17)°. These bond and angle parameters are close to those previously reported for complex $[Ru(bpy)_2(Hdpa)](BF_4)_2$ (Hdpa = dipyridin-2-ylamine).[11] The two pyridyl substituents of the dpa ligand are non-

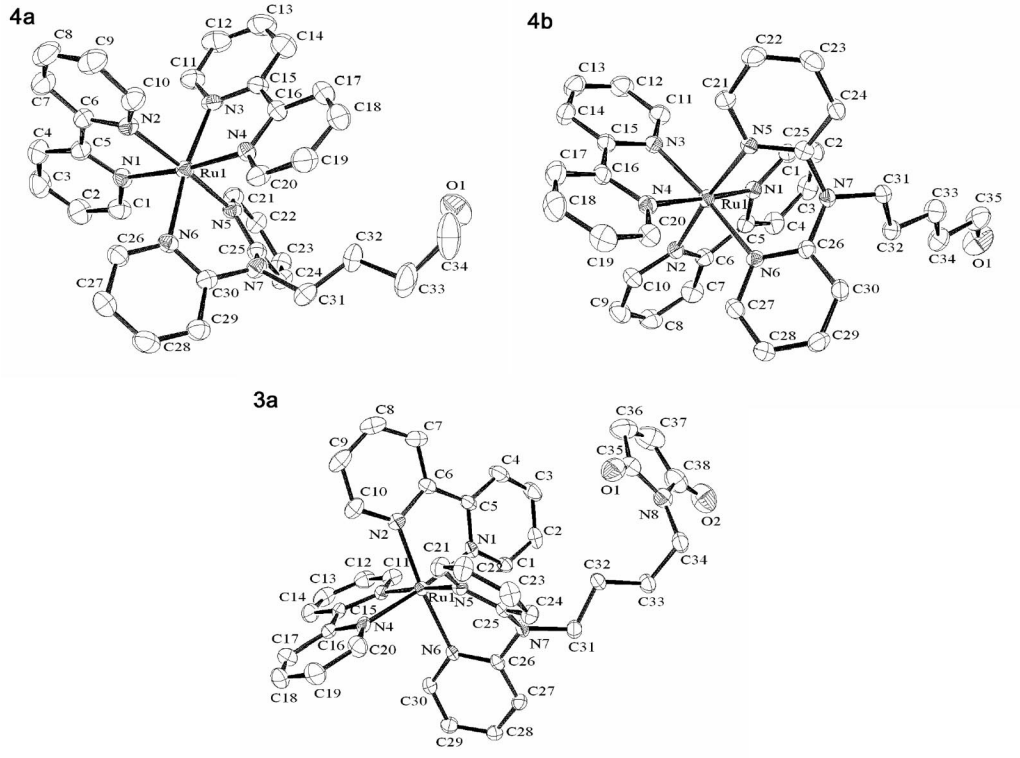

Figure 1. Molecular structures of **3a**, **4a** and **4b** (H atoms, PF_6^- counterions and CH_2Cl_2 molecules omitted for clarity). Ellipsoids are at the 50% probability level.

planar (angle between the 2 planes: 131° for **3a**, 129° for **4b**, 128° for **4a**). In the three structures, the geometry around the central nitrogen atom of the dpa ligands is close to planarity [C–N–C angles ranging from 116.4(4) to 119.9(3)°].

The chiral-at-metal complexes **3a**–**b** and **4a**–**b** display a C_2 axis in solution as revealed by their solution NMR spectra (Figures S1–S4). The protons from the equivalent bpy ligands appear as two sets of four signals, whereas those from the equivalent pyridyl moieties of the dpa ligand appear as a single set of four signals. Diastereotopic protons from the methylene group linked to the nitrogen atom of the dpa ligand give a pair of distinct triplets of doublets.

Photophysical Properties of the Ligands and Complexes

The absorption and emission spectra of the ligands and complexes were measured in air-equilibrated water at room temperature. The spectroscopic data are gathered in Table 1, and representative spectra of ligands and complexes are depicted in Figure 2.

Table 1. Spectroscopic and photophysical parameters of ligands and complexes. Data measured in air-equilibrated aqueous solutions at 20 °C.

	Absorption	Emission	
	λ_{max} [nm] (ε [L mol^{-1} cm^{-1}])	λ_{em} [nm]	Φ
1a	236 (8500), 275 (7700), 310 (9400)	406	0.0003
1b	232 (12000), 276 (7800), 310 (9900)	405	0.0008
2a	233 (8500), 275 (7100), 310 (8800)	371	0.0086
2b	275 (8100), 310 (9800)	373	0.0088
3a	287 (57400), 338 (10500), 463 (9200)	605	0.0027
3a+cys	287 (45400), 340 (9800), 462 (8700)	603	0.0097
3b	287 (71000), 462 (10500)	603	0.0021
4a	287 (55000), 340 (10100), 463 (8800)	605	0.0054
4b	287 (47000), 340 (8700), 463 (7600)	605	0.0053

Ligands **1a**–**b** and **2a**–**b** display very similar electronic absorption spectra in the UV region with two prominent bands at 310 and 275 nm, assigned to amine N-to-ring CT and pyridine-based (LC) transitions, respectively.[12,13] Ligands **1a**–**b** comprising the maleimide entity are only weakly luminescent, in contrast to ligands **2a**–**b** (**1b** is 10 times less fluorescent than **2b**) and other dipyridin-2-ylamine derivatives.[12,13] Maleimides have long been known to quench the fluorescence of fluorophores they are attached to,[7,14,15] but the mechanism involved in this quenching has been disclosed only recently.[15,16] The quenching mode was identified as photoinduced electron transfer. The fluorescence quantum yields of **2a** and **2b** are lower than those of Hdpa and previously reported *N*-substituted dpa ligands.[12,17]

The Ru^{II} complexes **3a**–**b** and **4a**–**b** display a characteristic absorption band around 460 nm corresponding to the MLCT transition d(Ru^{II}) → π* (bpy) and a shoulder around 340 nm corresponding to the MLCT transition d(Ru^{II}) → π* (dpa). The most intense absorption band is

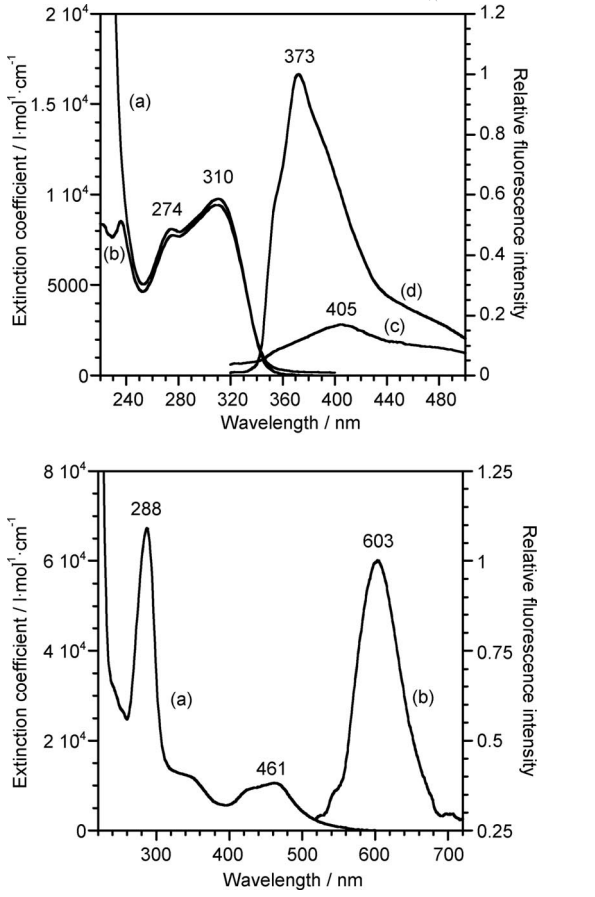

Figure 2. (Top) Absorption and emission spectra of ligands **1b** (a, c) and **2b** (b, d). Spectra recorded in air-equilibrated water at 20 °C (excitation at 310 nm for the luminescence spectra). (Bottom) Absorption (a) and emission (b) spectra of **3b**. Spectra recorded in air-equilibrated water at 20 °C (excitation at 460 nm for the luminescence spectrum).

observed at 287 nm and assigned to a ligand-centred (LC) transition.[18] The emission band centred at about 600 nm results from the MLCT transition dπ* from bpy to Ru^{III} as observed for $[Ru(bpy)_3]^{2+}$.[19] As previously observed for the ligands, the Ru^{II}–maleimide derivatives **3a**–**b** are less fluorescent than the alcohol derivatives **4a**–**b**, but only by a factor of about 2. Finally, the compound resulting from the reaction of **3a** with cysteine also displays an emission band at about 600 nm, but its quantum yield is multiplied by a factor of 3.6 with respect to **3a**.

Reaction of 1a–b and 3a–b with Papain and Conjugate Characterization

Papain is an enzyme of the cysteine endoproteinase family. It is made up of a single polypeptidic chain of 212 amino acids, 7 of which are cysteines. Six of these cysteines are involved in disulfide bridges, whereas the remaining cysteine residue (Cys25) is part of the active site and is essential for catalysis.[20] The particular folding of papain together with the presence of a reactive cysteine makes it an interesting protein to construct artificial metalloen-

zymes.[10,21] Any chemical modification of Cys25 will abolish papain's hydrolytic activity, making it easy to monitor the kinetics of its reaction with alkylating agents. In a typical experiment, papain was incubated with the maleimides in large excess (i.e., under pseudo-first-order rate conditions), and the hydrolytic activity of the mixtures was periodically measured on the chromogenic substrate PFLNa. The same experiment was also carried out with the alcohols **1b**, **4a** and **4b** at the same concentrations. Time-dependent decrease of enzymatic activity was only observed with the maleimides, whereas no inhibition was observed with the alcohol derivatives. Semi-logarithmic plots of initial PFLNa hydrolysis rates versus time are linear (see Figure S9) and give the pseudo-first-order rate constants k_{obs}, from which the second-order rate constants of inactivation k_{2nd} (Table 2) are calculated.

Table 2. Inactivation rate constants of papain by ligands and complexes measured in 20 mM phosphate, 400 mM NaCl, pH = 7, *F*/*P* ratios and ESI-MS analysis of conjugates.

	k_{2nd} [$M^{-1}min^{-1}$]	*F*/*P*	M [amu]	
			Calculated	Found
1a	3180 ± 70	0.9	23744	23762 ± 4
1b	1970 ± 70	1.4	23758	23769 ± 3
			24094	24104 ± 1
3a	5700 ± 550	1.1	24157	24170 ± 3
3b	2060 ± 40	0.9	24171	24184 ± 2

The molecule that inactivated papain the fastest was **3a**. Surprisingly, **3a** inactivated papain more quickly than the corresponding dpa ligand **1a**. In the 5-methylene spacer arm series, ligand **1b** and the Ru^{II} complex **3b** inactivated papain at the same rate. Within each family of molecules, there was a clear influence of the spacer arm length on the inactivation rate; the shorter arm yielded faster rates than the longer one. We had previously noticed such a trend for the (η^6-arene)Ru^{II} series of complexes.[9] This is rather surprising considering the bulkiness of the organometallic entities but may account for the nature of papain's active site, which is known to contain several nonpolar residues.

These experiments were repeated on a larger scale and the protein conjugates isolated by gel filtration chromatography or dialysis. As expected, none of these conjugates displayed enzymatic activity towards PFLNa. The absorption spectrum of the protein conjugates displays a major band around 280 nm assigned to the protein, with contributions from the species covalently bound to it. Other features are observed at higher wavelengths for the papain conjugates with **1a**–**b** and **3a**–**b**, corresponding to the absorption of the added chromophores, that is, a shoulder at 320 nm for the former and a band at 460 nm for the latter (Figure 3). The *F*/*P* ratio of the protein conjugates, that is, the number of fluorophores coupled per protein molecule, is calculated from their UV/Vis spectra, taking papain and the maleimide reagents as standard compounds (Table 2). *F*/*P* ratios around 1 were determined for the protein conjugates, except for **1b**, for which it is higher.

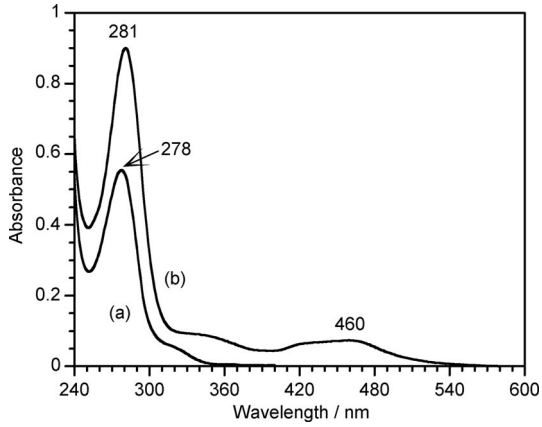

Figure 3. Absorption spectra of PAP-**1a** (a) and PAP-**3a** (b).

The protein conjugates were further submitted to ESI-MS analysis (Table 2). For **1a** and **3a**–**b**, the mass spectrum of the conjugates exhibits one series of peaks corresponding to a mass 10–18 amu higher than the calculated mass of the 1:1 conjugates (Figures S5–S8). This confirmed that the bioconjugates resulted from the covalent binding of one ligand/complex per protein molecule. The additional 18 amu found in the case of papain-**1a** may be due to the ring opening of the succinimidyl thioether (resulting from the reaction of the thiol with the maleimide) by addition of a molecule of water. Indeed, maleimide bioconjugates can undergo spontaneous hydrolysis to yield isomeric succinamic acid thioethers.[22] For **1b**, the ESI mass spectrum of the conjugate exhibits a second series of peaks corresponding to a mass of (24104 ± 1) amu, assigned to a 2:1 protein conjugate. This explains why the *F*/*P* ratio is higher than 1 for this particular bioconjugate. From this set of data, we concluded that bioconjugates PAP-**1a**, -**3a** and -**3b** resulted from the selective and covalent binding of **1a**, **3a** and **3b** to the active-site cysteine residue of papain, whereas bioconjugate PAP-**1b** was a mixture of proteins labelled at different residues, including Cys25. Therefore, the next experiments were carried out exclusively with PAP-**1a**, PAP-**3a** and PAP-**3b**.

Fluorescence spectra of the protein conjugates were recorded at two different excitation wavelengths: (a) at 280 nm where the protein aromatic residues absorb and (b) at 310 or 460 nm where the polypyridyl ligands or the (polypyridyl)Ru^{II} complexes absorb. The photophysical data for the papain conjugates are listed in Table 3.

Table 3. Photophysical parameters of the papain conjugates in aerated aqueous solution at 20 °C.

	λ_{max} [nm]	λ_{em} [nm]	Φ[a]
PAP-**1a**	278, 310 (sh)	347,[b] 370[c]	0.02
PAP-**3a**	281, 320 (sh), 460	329,[b] 598[d]	0.034
PAP-**3b**	281, 320 (sh), 460	333,[b] 600[d]	0.03

[a] At λ_{em} = 600 nm. [b] λ_{ex} = 280 nm. [c] λ_{ex} = 310 nm. [d] λ_{ex} = 460 nm.

When excitation was carried out at 280 nm, all the protein conjugates displayed typical protein fluorescence emission around 340 nm owing to the aromatic residues (tyrosine and tryptophan), but the position of the maximum depended on the conjugated molecule. For the papain–**1a** conjugate, the emission maximum was shifted to the red by 9 nm with respect to the native protein (λ_{em} = 338 nm under our measurement conditions) with simultaneous enhancement of the fluorescence (Figure 4).

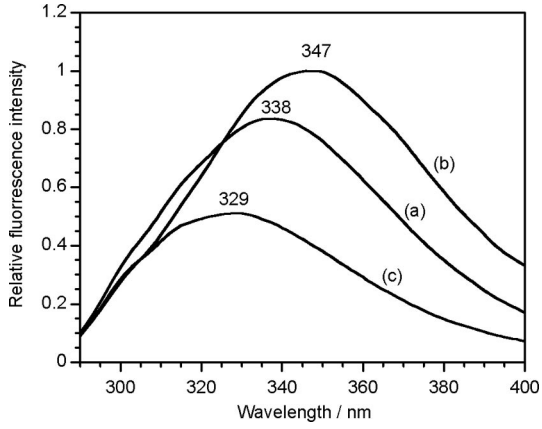

Figure 4. Emission spectra of aqueous solutions of papain (a), PAP-**1a** (b) and PAP-**3a** (c) at 0.5 μM. Excitation at 280 nm.

These changes are probably due to the additional contribution of the coupled dipyridin-2-ylamine moiety to the emission (λ_{em} = 370 nm). Conversely, the emission maximum of the papain–**3a** and papain–**3b** conjugates was shifted to the blue by 9 or 5 nm, respectively. In the case of papain–**3a**, this was accompanied by a quenching of the fluorescence by 40% with respect to the unmodified protein (Figure 4). Such a shift normally indicates that some tryptophan residues become located in a more hydrophobic environment.[23] According to Schechter and Berger, the catalytic site of papain comprises 7 subsites denoted S_1–S_4 and S'_1–S'_3, each accommodating an amino acid residue of the substrate.[24] X-ray structural studies later confirmed this finding and allowed location of the 5 tryptophanes included in the sequence.[20] Four of these tryptophanes (W26, W69, W177 and W181) are actually located close to Cys25, where the ligands/complexes are anchored. W177 and W181 are on the S′ side of the catalytic site, whereas W69 is located at the far end of the S side of the catalytic site. Interestingly, X-ray structural analyses revealed that two irreversible inhibitors of papain closely interacted with Trp177 by π-stacking of an aromatic group of the inhibitor.[25] It might be possible that such an interaction occurs between papain and **3a**–**b**. When excitation was carried out at 310 nm, the papain–**1a** conjugate displayed a strong emission at 370 nm readily associated to the dipyridin-2-ylamine fluorophore. This position is identical to that observed for ligand **2b**, which lacks the maleimide group. This confirmed that **1a** is bound to papain as a result of the addition of the thiol of Cys25 to the double bond of the maleimide group. The quantum yield of the ligand fluorophore covalently bound to papain was higher than that of **2b** by a factor of 2.

When excitation was carried out at 460 nm, the conjugates of papain with the (polypyridyl)Ru^{II} complexes displayed a typical emission band at 600 nm. Thus, the protein acquired the emission feature of the Ru^{II} fluorophores. The presence of the protein environment did not influence the position of the emission maximum, but it noticeably enhanced the quantum yield of the fluorophores with respect to the starting materials **3a**–**b**. The factor of enhancement was equal to 13 for **3a** and 14 for **3b**. Part of this enhancement was due to the conversion of maleimide to succinimide (factor of 3.6, see Table 1). Still, the protein environment around the fluorophores enhanced their emission by a factor of about 4. Several hypotheses may be put forward to explain this additional emission enhancement. First, the presence of the protein core may enhance the luminescence of the polypyridyl Ru^{II} fluorophores by placing them in a hydrophobic environment. This is unlikely, because no correlation between the intensity of emission of **4a** (nor the position) and the dielectric constant of various solvents was observed (see Figure S10). Second, the luminescence of polypyridyl Ru^{II} complexes is known to be sensitive to the presence of ambient dioxygen. Indeed, some $[Ru(bpy)_2(N–N)]^{2+}$ probes have been shown to undergo a quenching of emission intensity of 40% in the presence of dioxygen.[5] However, covalent attachment of polypyridyl Ru^{II} probes to proteins noticeably reduced the sensitivity of the probe to oxygen quenching, because the protein environment exerted a shielding towards oxygen. Similarly, it was also observed that binding of a polypyridyl Ru^{II} derivative of biotin to streptavidin enhanced the luminescence of the probe by shielding it from dissolved dioxygen.[26] By analogy, the position of the anchoring group within the enzyme's active site could place the probes in such an environment that they may be at least partially protected against O_2 quenching. Indeed, the emission intensity of **3b** was quenched by 30% in the presence of dioxygen, whereas that of PAP-**3b** was quenched by only 12%. Nevertheless, this shielding mechanism cannot totally account for the emission enhancement factor observed. Third, it appears that the emission spectrum of papain overlaps the absorption spectrum of **3a**–**b**. This may favour a resonance energy transfer (RET) phenomenon between the protein aromatic residue(s) acting as the donor(s) and the probe acting as the acceptor, providing the distance between donor(s) and acceptor is compatible.[27] This assumption is supported by the fact that actual quenching of the papain luminescence is observed simultaneously (Figure 4). Such an RET phenomenon between some of the Trp residues and a fluorescent probe was previously observed in the case of the tight-binding inhibitor mansyl-Phe-glycinal in complex to papain.[28] Thus, we conclude that the luminescence enhancement of **3a**–**b** covalently bound to papain is probably due to a combination of three factors: (1) conversion of maleimide to succinimide, (2) partial probe shielding towards O_2 and (3) moderate RET between the protein aromatic residues and the probe.

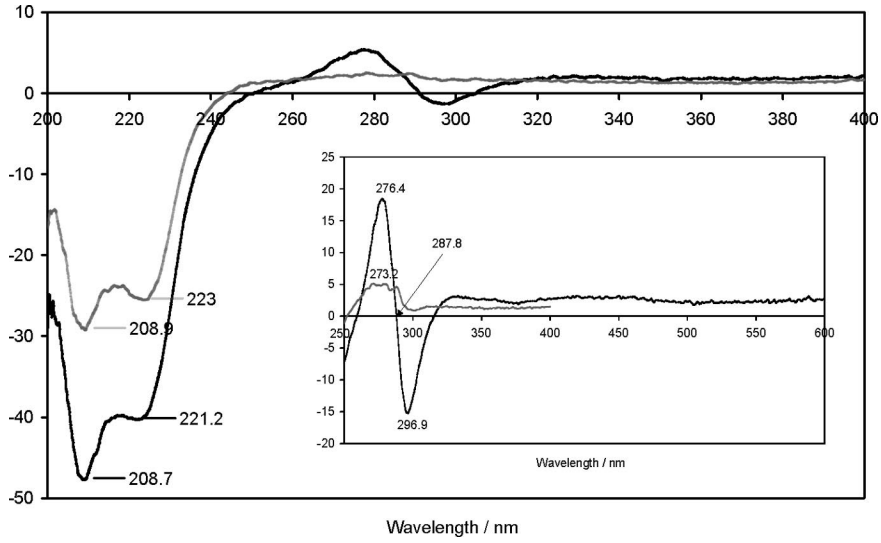

Figure 5. CD spectra of native papain (light grey trace) and papain–**3a** conjugate (black trace) at 8.8 μM and 44 μM (inset) in 0.15 M NaCl.

Finally, the circular dichroism (CD) spectrum of the papain–**3a** conjugate was recorded together with that of unmodified papain (Figure 5). In the far-UV range, the CD spectra of papain and papain–**3a** both displayed two negative bands at 209 and 223 nm that are characteristic of the α-helix motives of the protein.[29] This indicated that the protein folding was globally undisturbed by covalent binding of the polypyridyl Ru^{II} complex. Nevertheless, the bands were more intense in the case of the protein–Ru^{II} conjugate. Conversely, new features were observed in the near-UV range in the case of the papain–**3a** conjugate (Figure 5, inset). Whereas the CD spectrum of papain displayed a weak positive band centred at 273 nm associated to its aromatic residues,[30] the papain–**3a** conjugate displayed a bisignate band with extrema at 276 and 297 nm, zero crossing at 287 nm and a negative Cotton effect that is very similar to that observed for the Δ enantiomer of $[Ru(diimine)_3]^{2+}$ complexes.[18,31] This indicated that, although papain was allowed to react with complex **3a** in its racemic form, the Michael addition proceeded in a stereoselective fashion, and only the Δ form of the complex eventually bound to the protein. Chiral discrimination between enantiomers of bis(dipyridin-2-ylamine)Ru^{II} complexes upon interaction with DNA in favour of the Δ isomer was previously noticed,[32] but this is the first time to the best of our knowledge that such a discrimination has occurred upon covalent binding of such complexes to a protein.

Conclusions

Two luminescent polypyridyl Ru^{II} complexes including dipyridin-2-ylamine ligands functionalized by a maleimide group were synthesized and characterized, and the photophysical properties of these complexes together with the starting dipyridin-2-ylamine ligands were disclosed. Reaction of the ligands and the complexes with the cysteine endoproteinase papain was shown to occur at the single free cysteine (Cys25) as expected by the usual reactivity of maleimides. The resulting bioconjugates displayed luminescence that was typical of the fluorophore attached to the protein, and luminescence enhancement was observed with respect to the starting reagents. Finally, reaction of papain with one of the *rac* complexes appeared to be stereoselective in favour of the Δ enantiomer, as observed by the appearance on the CD spectrum of the bioconjugate of a typical bisignate band in the near-UV range.

Experimental Section

Materials: Solvents were dried and distilled by standard procedures, and all reactions and manipulations were performed under an argon or nitrogen by using standard Schlenk and vacuum-line techniques. Flash chromatography was performed on silica gel Merck 60 (40–63 μm). NMR spectra were recorded with a 300 MHz Bruker spectrometer. High-resolution mass spectra were recorded with an MStation JMS 700 (Jeol). $[Ru(bpy)_2Cl_2]$ was synthesized according to a published procedure.[33] Ligands **1a**–**b** and **3a**–**b** were prepared according to our published procedure.[9] Papain (reference 76220) was purchased from Fluka and purified by affinity chromatography as described previously.[34] Catalytic activities were measured with L-pyroglutamyl-L-phenylalanyl-L-leucine-*p*-nitroanilide PFLNa (Bachem).[35]

Methods

General Procedure for the Synthesis of the (polypyridyl)Ru^{II} Complexes: $[Ru(bpy)_2Cl_2]$ (0.05 g, 0.096 mmol) and ligand (0.125 mmol; 1.3 equiv.) were refluxed in ethanol (10 mL) for 16 h. The solvent was evaporated under reduced pressure. The crude solid was then dissolved in a minimum of water. Upon addition of ammonium hexafluorophosphate (2 equiv.), the complex precipitated as an orange-red powder. The solid was dissolved in a minimum of CH_2Cl_2 and precipitated again when poured into 100 mL of *n*-hexane.

3a: Yield 0.09 g (91%). ^{1}H NMR (300 MHz, [D$_6$]acetone, 25 °C): δ = 8.84 (d, $^3J_{H,H}$ = 8.1 Hz, 2 H, H$_{Py}$), 8.75 (d, $^3J_{H,H}$ = 7.9 Hz, 2 H, H$_{Py}$), 8.61–8.53 (m, 2 H, H$_{Py}$), 8.34–8.29 (m, 2 H, H$_{Py}$), 8.14–8.08 (m, 2 H, H$_{Py}$), 8.03–7.94 (m, 4 H, H$_{Py}$), 7.80–7.65 (m, 6 H, H$_{Py}$), 7.51–7.47 (m, 2 H, H$_{Py}$), 7.08–7.04 (m, 2 H, H$_{Py}$), 6.92 (s, 2 H, N–CH=C), 4.50–4.40 (m, 1 H, CH$_2$), 4.01–3.92 (m, 1 H, CH$_2$), 3.43–3.35 (m, 2 H, CH$_2$), 1.67–1.48 (m, 3 H, CH$_2$), 0.69–0.52 (m, 1 H, CH$_2$) ppm. ^{13}C NMR (75 MHz, [D$_6$]acetone, 25 °C): δ = 171.7, 159.2, 158.6, 158.5, 154.0, 152.6, 151.9, 140.4, 138.9, 138.5, 135.3, 128.5, 128.3, 125.5, 125.3, 122.2, 118.8, 51.9, 37.6, 26.9, 25.0 ppm. HRMS: calcd. for $C_{38}H_{34}N_8O_2Ru^{2+}$ 368.09240; found 368.09186.

3b: Yield 0.09 g (90%). ^{1}H NMR (300 MHz, [D$_6$]acetone, 25 °C): δ = 8.83 (d, $^3J_{H,H}$ = 8.1 Hz, 2 H, H$_{Py}$), 8.74 (d, $^3J_{H,H}$ = 8.1 Hz, 2 H, H$_{Py}$), 8.62–8.55 (m, 2 H, H$_{Py}$), 8.33–8.28 (m, 2 H, H$_{Py}$), 8.14–8.08 (m, 2 H, H$_{Py}$), 8.02–7.94 (m, 4 H, H$_{Py}$), 7.82–7.62 (m, 6 H, H$_{Py}$), 7.51–7.46 (m, 2 H, H$_{Py}$), 7.08–7.03 (m, 2 H, H$_{Py}$), 6.90 (s, 2 H, N–CH=C), 4.42–4.32 (m, 1 H, CH$_2$), 3.98–3.88 (m, 1 H, CH$_2$), 3.51–3.38 (m, 2 H, CH$_2$), 1.65–1.30 (m, 5 H, CH$_2$), 0.72–0.55 (m, 1 H, CH$_2$) ppm. ^{13}C NMR (75 MHz, [D$_6$]acetone, 25 °C): δ = 171.8, 159.2, 158.6, 158.5, 154.0, 152.6, 151.8, 140.4, 138.8, 138.4, 135.2, 128.4, 128.3, 125.6, 125.3, 122.2, 118.8, 52.3, 37.8, 28.7, 27.0, 24.7 ppm. HRMS: calcd. for $C_{39}H_{36}N_8O_2Ru^{2+}$ 375.10024; found 375.09969.

4a: Yield 0.081 g (89%). ^{1}H NMR (300 MHz, [D$_6$]acetone, 25 °C): δ = 8.82 (d, $^3J_{H,H}$ = 8.1 Hz, 2 H, H$_{Py}$), 7.74 (d, $^3J_{H,H}$ = 8.1 Hz, 2 H, H$_{Py}$), 8.63–8.55 (m, 2 H, H$_{Py}$), 8.33–8.27 (m, 2 H, H$_{Py}$), 8.14–8.09 (m, 2 H, H$_{Py}$), 8.03–7.95 (m, 4 H, H$_{Py}$), 7.82–7.64 (m, 6 H, H$_{Py}$), 7.52–7.47 (m, 2 H, H$_{Py}$), 7.08–7.04 (m, 2 H, H$_{Py}$), 4.48–4.34 (m, 1 H, CH$_2$), 4.02–3.88 (m, 1 H, CH$_2$), 3.56–3.44 (m, 2 H, CH$_2$), 1.70–1.49 (m, 3 H, CH$_2$), 0.76–0.59 (m, 1 H, CH$_2$) ppm. ^{13}C NMR (75 MHz, [D$_6$]acetone, 25 °C): δ = 159.2, 158.6, 158.4, 153.9, 152.5, 151.7, 140.2, 138.7, 138.3, 128.3, 128.2, 125.4, 125.2, 122.0, 118.8, 61.6, 52.4, 30.7, 24.3 ppm. HRMS: calcd. for $C_{34}H_{33}N_7ORu^{2+}$ 328.58937; found 328.58896.

4b: Yield 0.086 g (93%). ^{1}H NMR (300 MHz, [D$_6$]acetone, 25 °C): δ = 8.82 (d, $^3J_{H,H}$ = 8.1 Hz, 2 H, H$_{Py}$), 7.73 (d, $^3J_{H,H}$ = 8.1 Hz, 2 H, H$_{Py}$), 8.63–8.54 (m, 2 H, H$_{Py}$), 8.33–8.28 (m, 2 H, H$_{Py}$), 8.13–8.07 (m, 2 H, H$_{Py}$), 8.02–7.93 (m, 4 H, H$_{Py}$), 7.81–7.63 (m, 6 H, H$_{Py}$), 7.51–7.46 (m, 2 H, H$_{Py}$), 7.08–7.03 (m, 2 H, H$_{Py}$), 4.46–4.33 (m, 1 H, CH$_2$), 3.98–3.83 (m, 1 H, CH$_2$), 3.53–3.44 (m, 2 H, CH$_2$), 1.60–1.38 (m, 5 H, CH$_2$), 0.64–0.51 (m, 1 H, CH$_2$) ppm. ^{13}C NMR (75 MHz, [D$_6$]acetone, 25 °C): δ = 159.1, 158.5, 158.4, 153.9, 152.5, 151.7, 140.2, 138.7, 138.3, 128.3, 128.2, 125.4, 125.1, 122.0, 118.7, 61.9, 52.4, 32.9, 27.3, 24.1 ppm. HRMS: calcd. for $C_{35}H_{35}N_7ORu^{2+}$ 335.59714; found 335.59678.

X-ray Crystallography: Single crystals of complexes **3a**, **4a** and **4b** were mounted on a Nonius Kappa-CCD area detector diffractometer (Mo-K_α, λ = 0.71073 Å). The complete conditions of data collection (Denzo software)[36] and structure refinements are gathered in Table S1 (Supporting Information). The cell parameters were determined from reflections taken from one set of 10 frames (1.0° steps in ϕ angle), each at 20 s exposure. All the structures were solved by direct methods (SHELXS97) and refined against F^2 by using the SHELXL97 software.[37] The absorption was not corrected. All non-hydrogen atoms were refined anisotropically. Hydrogen atoms were generated according to stereochemistry and refined by using a riding model in SHELXL97. In complex **4a**, one of the PF_6^- anions is disordered over two positions. CCDC-776931 (for **3b**), -776932 (for **3a**) and -776933 (for **4b**) contain the supplementary crystallographic data for this paper. These data can be obtained free of charge from The Cambridge Crystallographic Data Centre via www.ccdc.cam.ac.uk/data_request/cif.

Kinetics of Inactivation of Papain by Ligands and Complexes: Papain (4.2 μM) and the compound to be tested (50 μM for **3a**–**b**; 100 μM for **1a**–**b**) were incubated at room temperature in a 20 mM phosphate 0.4 M NaCl (pH = 7.0)/dmso (95:5) mixture (final volume 100 μL). At defined time intervals, an aliquot (15 μL) was dispensed in duplicate into wells of a 96-well microtitre plate (Greiner), and the substrate (135 μL; 0.111 mM in assay buffer/dmso, 8:1) was added to the wells. The OD_{415nm} was immediately monitored for 2 min with a microtitre plate reader (Biorad model 680).

Conjugation of 1a to Papain: Papain [4.9 μM in 20 mM phosphate 0.4 M NaCl (pH = 7); 20 mL] was mixed with **1a** (2 mg, 6.1 μmol, 60 equiv.), and the mixture was incubated at room temp. for 24 h. The mixture was concentrated to 4 mL by ultrafiltration in a 50 mL stirred cell equipped with a 5 kD Ultracell membrane (Millipore) then dialyzed in water at 4 °C for 24 h. The conjugate solution was finally concentrated to 1 mL with an Amicon Ultra-15 10 K centrifugal filter device (Millipore). The *F*/*P* ratio was calculated from absorbance measurements at 280 nm [ε(pap) = 57600; ε(**1a**) = 7800] and 320 nm [ε(**1a**) = 8700].

Conjugation of 1b to Papain: Papain [6.6 μM in 20 mM phosphate 0.4 M NaCl (pH = 7); 4.5 mL] was mixed with **1b** (2 mM in dmso; 0.5 mL, 30 equiv.) and the solution incubated at room temp. overnight, then passed on a gel filtration column (Hiprep 26/10 desalting, GE Healthcare) by using 0.15 M NaCl as eluent at 5 mL min^{-1} to remove excess reagent. The conjugate solution was concentrated to 1 mL by ultrafiltration in a 50 mL stirred cell equipped with a 5 kD Ultracell membrane (Millipore) then dialyzed in water to remove NaCl. The *F*/*P* ratio was calculated from absorbance measurements at 280 nm [ε(pap) = 57600; ε(**1b**) = 7700] and 320 nm [ε(**1b**) = 8400].

Conjugation of 3a–b to Papain: Papain [7.5 μM in 20 mM phosphate 0.4 M NaCl (pH = 7); 10 mL] was mixed with **3a** or **3b** (1 mM in dmso, 0.75 mL, 10 equiv.), and solutions were incubated at room temp. overnight without stirring. The enzymatic activity of the solutions on PFLNa was checked, then they were passed on a gel filtration column (Hiprep 26/10 desalting, GE Healthcare) by using 0.15 M NaCl as eluent at 5 mL min^{-1} to remove excess reagent. The conjugate solutions were concentrated to 2 mL by ultrafiltration in a 50 mL stirred cell equipped with a 5 kD Ultracell membrane (Millipore). A fraction of these solutions (0.5 mL) was dialyzed in water to remove NaCl and further concentrated to 50 μL with an Amicon Ultra-0.5 5 kD centrifugal filter (Millipore) to obtain suitable samples for ESI-MS analysis. The *F*/*P* ratios were calculated from absorbance measurements at 280 nm [ε(pap) = 57600; ε(**3a**–**b**) = 55000] and 460 nm [ε(**3a**) = 9200; ε(**3b**) = 10500].

Spectroscopic Analyses: Absorption spectra of aqueous solutions of ligands, complexes and papain conjugates were recorded with a UV/mc2 spectrophotometer (Safas). Fluorescence spectra of air-equilibrated aqueous solutions of ligands, complexes and conjugates were recorded with an FP-6200 spectrofluorimeter (Jasco) equipped with a Peltier thermostatted cell holder. All luminescence spectra were recorded at (20 ± 0.1) °C. Quantum yields were measured according to the comparative method of Williams et al.[38] by using $[Ru(bpy)_3]Cl_2$ (Φ = 0.028 in air-aerated solution, excitation at 455 nm)[39] or tryptophan (Φ = 0.14 in water, excitation at 280 nm)[40] as standard samples. Circular dichroism spectra were recorded with a J-815 CD spectrometer (Jasco) at (20 ± 0.1) °C by using a quartz cell with an optical pathlength of 0.2 cm (Starna scientific). ESI mass spectra were acquired with a triple quadrupole

mass spectrometer API 3000 LC-MS/MS system (Applied Biosystems, PE Sciex) in positive-ion mode with the following parameters: declustering potential 20 V, capillary voltage 5000 V, source temperature 400 °C. Samples (80 μM, 20 μL) acidified with 10% formic acid (5 μL) were introduced through the liquid chromatography system (Agilent 1100 series) without column into the turbo ion spray source by using H_2O/MeOH (1:1) as eluent (0.2 mL min^{-1}). The molecular masses were calculated from *m/z* peaks in the charge distribution profile of the multiply charged ions with Hypermass 11 script of Analyst 1.1 software (Applied Biosystems, PE Sciex). Mass spectra were deconvoluted with the MagTran 1.03 software.[41]

Supporting Information (see footnote on the first page of this article): Crystallographic data and selected bond lengths and angles (2 tables); ^{1}H and ^{13}C NMR spectra of **3a**–**b** and **4a**–**b** (8 figures); kinetic plots of irreversible inhibition by **1a**–**b** and **3a**–**b** (4 figures). ESI mass spectra of papain-**1a**, papain-**1b**, papain-**3a** and papain-**3b** (4 figures); solvent effect on the fluorescence emission of **4b** (1 figure).

Acknowledgments

The Centre National de la Recherche Scientifique (CNRS) and the French Ministry of Research are gratefully acknowledged for financial support. Dr. Christophe Desmarets is acknowledged for allowing access to the CD equipment of the Institut Parisien de Chimie Moléculaire (Université Pierre et Marie Curie, Paris, France). Dr. Lydia Brelot is also thanked for her help in the X-ray crystallographic studies of complexes **3b**, **4a** and **4b**.

[1] G. Piszczek, *Arch. Biochem. Biophys.* **2006**, *453*, 54–62; A. Coleman, C. Brennan, J. G. Vos, M. T. Pryce, *Coord. Chem. Rev.* **2008**, *252*, 2585–2595; A. Juris, V. Bolzani, F. Barigelleti, S. Campagna, P. Belsa, A. von Zelewsky, *Coord. Chem. Rev.* **1988**, *84*, 85–277.
[2] J. R. Lakowicz, *Principles of Fluorescence Spectroscopy*, Springer, New York, **2006**, pp. 675–703.
[3] A. B. Tossi, J. M. Kelly, *Photochem. Photobiol.* **1989**, *49*, 545–556.
[4] G. T. Hermanson, *Bioconjugate Techniques*, Academic Press, London, **2008**.
[5] F. N. Castellano, J. D. Dattelbaum, J. R. Lakowicz, *Anal. Biochem.* **1998**, *255*, 165–170; E. Terpetschnig, J. D. Dattelbaum, H. Szmacinsky, J. R. Lakowicz, *Anal. Biochem.* **1997**, *251*, 241–245.
[6] R. C. Lasey, S. S. Banerji, M. Y. Ogawa, *Inorg. Chim. Acta* **2000**, *300–302*, 822–828; S. A. Trammell, S. D. Jhaveri, S. R. LaBrenz, J. M. Mauro, *Biosens. Bioelectron.* **2003**, *19*, 373–382; F. Millett, B. Durham, *Methods Enzymol.* **2009**, *456*, 95–109; L. M. Geren, J. R. Beasley, B. R. Fine, A. J. Saunders, S. Hibdon, G. J. Pielak, B. Durham, F. Millett, *J. Biol. Chem.* **1995**, *270*, 2466–2472; G. Engstrom, R. Rajagukguk, A. J. Saunders, C. N. Patel, S. Rajagukguk, T. Merbitz-Zahradnik, K. H. Xiao, G. J. Pielak, B. Trumpower, C. A. Yu, L. Yu, B. Durham, F. Millett, *Biochemistry* **2003**, *42*, 2816–2824.
[7] J. Weh, A. Duerkop, O. S. Wolfbeis, *ChemBioChem* **2007**, *8*, 122–128.
[8] S. R. Banerjee, J. W. Babich, J. Zubieta, *Chem. Commun.* **2005**, 1784–1786; S. R. Banerjee, P. Schaffer, J. W. Babich, J. F. Valliant, J. Zubieta, *Dalton Trans.* **2005**, 3886–3897; J. D. Dattelbaum, O. O. Abugo, J. R. Lakowicz, *Bioconjugate Chem.* **2000**, *11*, 533–536; K. K.-W. Lo, W.-K. Hui, D. C.-M. Ng, K.-K. Cheung, *Inorg. Chem.* **2002**, *41*, 40–46.
[9] P. Haquette, B. Dumat, B. Talbi, S. Arbabi, J.-L. Renaud, G. Jaouen, M. Salmain, *J. Organomet. Chem.* **2009**, *694*, 937–941.
[10] B. Talbi, P. Haquette, A. Martel, F. de Montigny, C. Fosse, S. Cordier, T. Roisnel, G. Jaouen, M. Salmain, *Dalton Trans.* **2010**, *39*, 5605–5607.
[11] M. G. B. Drew, S. Nag, D. Datta, *Inorg. Chim. Acta* **2008**, *361*, 417–421.
[12] N. M. Shavaleev, A. Barbieri, Z. R. Bell, M. S. Ward, F. Barigelleti, *New J. Chem.* **2004**, *28*, 398–405.
[13] P. Jana, T. Ganguly, S. K. Sarkar, A. Mitra, P. K. Mallick, *J. Photochem. Photobiol., A* **1996**, *94*, 113–118.
[14] J. K. Weltman, R. P. Szaro, A. R. Frackelton Jr., R. M. Dowben, J. R. Bunting, R. E. Cathou, *J. Biol. Chem.* **1973**, *248*, 3173–3177; S. Girouard, M. H. Houle, A. Grandbois, J. W. Keillor, S. W. Michnick, *J. Am. Chem. Soc.* **2005**, *127*, 559–566.
[15] T. Matsumoto, Y. Urano, T. Shoda, H. Kojima, T. Nagano, *Org. Lett.* **2007**, *9*, 3375–3377.
[16] J. Guy, K. Caron, S. Dufresne, S. W. Michnick, W. G. Skene, J. W. Keillor, *J. Am. Chem. Soc.* **2007**, *129*, 11969–11977.
[17] M. R. McDevitt, Y. Ru, A. W. Addison, *Transition Met. Chem.* **1993**, *18*, 197–204.
[18] D. Hesek, Y. Inoue, S. R. L. Everitt, H. Ishida, M. Kunieda, M. G. B. Drew, *Inorg. Chem.* **2000**, *39*, 308–316.
[19] D. E. Morris, Y. Ohsawa, D. P. Segers, K. DeArmond, K. W. Hanck, *Inorg. Chem.* **1984**, *23*, 3010–3017.
[20] J. Drenth, J. N. Jansonius, R. Koekoek, B. G. Wolthers, *Adv. Protein Chem.* **1971**, *25*, 79–115.
[21] L. Panella, J. Broos, J. Jin, M. W. Fraaije, D. B. Janssen, M. Jeromius-Stratingh, B. L. Feringa, A. J. Minnaard, J. G. de Vries, *Chem. Commun.* **2005**, 5656–5658; M. T. Reetz, M. Rentzsch, A. Pletsch, M. Maywald, *Chimia* **2002**, *56*, 721–723; M. T. Reetz, M. Rentzsch, A. Pletsch, M. Maywald, P. Maiwald, J. J.-P. Peyralans, A. Maichele, Y. Fu, N. Jiao, F. Hollmann, R. Mondière, A. Taglieber, *Tetrahedron* **2007**, *63*, 6404–6414.
[22] J. Kalia, R. T. Raines, *Bioorg. Med. Chem. Lett.* **2007**, *17*, 6286–6289.
[23] E. A. Permyakov, *Luminescent Spectroscopy of Proteins*, CRC Press, Boca Raton, **1993**.
[24] I. Schechter, A. Berger, *Biochem. Biophys. Res. Commun.* **1967**, *27*, 157–162.
[25] J. Drenth, K. H. Kalk, H. M. Swen, *Biochemistry* **1976**, *15*, 3731–3738; H. Tsuge, T. Nishimura, Y. Tada, T. Asao, D. Turk, V. Turk, N. Katunuma, *Biochem. Biophys. Res. Commun.* **1999**, *266*, 411–416.
[26] T. Soller, M. Ringler, M. Wunderlich, T. A. Klar, F. Feldmann, H. P. Josel, J. Koci, Y. Markert, A. Nichtl, K. Kurzinger, *J. Phys. Chem. B* **2008**, *112*, 12824–12826.
[27] P. R. Selvin, S. Kenneth, *Methods Enzymol.* **1995**, *246*, 300–334.
[28] J. B. Henes, J. A. Mattis, J. S. Fruton, *Proc. Natl. Acad. Sci. USA* **1979**, *76*, 1131–1134.
[29] R. W. Woody, S. Kenneth, *Methods Enzymol.* **1995**, *246*, 34–71.
[30] A. O. Barel, A. N. Glazer, *J. Biol. Chem.* **1969**, *244*, 268–273.
[31] B. Bosnich, *Inorg. Chem.* **1968**, *7*, 2379–2386; X. Hua, A. von Zelewsky, *Inorg. Chem.* **1995**, *34*, 5791–5797; P. S. Braterman, B. C. Noble, R. C. Peacok, *J. Phys. Chem.* **1986**, *90*, 4913–1915.
[32] V. Rajendiran, M. Murali, E. Suresh, M. Palanuandavar, V. Subbarayan Periasamy, M. Abdulkader Akbarsha, *Dalton Trans.* **2008**, 2157–2170.
[33] B. P. Sullivan, D. J. Salmon, T. J. Meyer, *Inorg. Chem.* **1978**, *17*, 3334–3341.
[34] M. O. Funk, Y. Nakagawa, J. Skochdopole, E. T. Kaiser, *Int. J. Pept. Protein Res.* **1979**, *13*, 296–303.
[35] I. Y. Filippova, E. N. Lysogorskaya, E. S. Oksenoit, G. N. Rudenskaya, V. M. Stepanov, *Anal. Biochem.* **1984**, *143*, 293–297.
[36] *Kappa CCD Operation Manual*, Nonius, Delft, the Netherlands, **1997**.
[37] G. M. Sheldrick, *SHELXL97, Program for the Refinement of Crystal Structures*, Göttingen, Germany, **1997**.

[38] A. T. R. Williams, S. A. Winfield, J. N. Miller, *Analyst* **1983**, *108*, 1067–1071.
[39] K. Nakamura, *Bull. Chem. Soc. Jpn.* **1982**, *55*, 2697–2705.
[40] E. P. Kirby, R. F. Steiner, *J. Phys. Chem. B* **1970**, *74*, 4480–4490.
[41] Z. Zhang, A. G. Marshall, *J. Am. Chem. Soc. Mass Spectrom.* **1998**, *9*, 225–233.

Received: May 26, 2010
Published Online: September 24, 2010

